Collisional Quenching of Excited Electronic Species and the Parmenter et al. Correlation†

Chieu Nguyen Xuan*

Istituto di Metodologie Inorganiche e dei Plasmi, Consiglio Nazionale delle Ricerche, Area della Ricerca di Roma 1, Via Salaria Km 29,300, 00016 Monterotondo Scalo (Roma), Italy

Received: April 16, 2009; Revised Manuscript Received: August 3, 2009

The model of collision-induced deactivation of excited species proposed by Parmenter and co-workers has been examined in its application to the collisional quenching of $PH_2(\tilde{A}^2A_1)$. The correlation between the quenching efficiency and the molecular properties of the quenchers is seen to be closely obeyed only by rare gases and two molecules, H_2 and CH_4. The other molecular quenchers, conversely, show only a very loose trend of variation with the quantity ε_{M-M}, well depth of the potential between two molecules of the quencher M, which constitutes the basis for application of the Parmenter et al. model. This apparent limited validity of the Parmenter et al. correlation has been ascribed to the fact that the combining rule applied to the well depth $\varepsilon_{PH_2^*-M}$ of the collision complex PH_2^*-M to express this quantity as $(\varepsilon_{PH_2^*-PH_2^*})^{1/2}(\varepsilon_{M-M})^{1/2}$ is applicable only to rare gases and not to most of the other quenchers. A procedure to find the charateristics of rare gas-like molecules with quenching efficiencies equal to those of the real quenchers has been proposed. A plot of the quenching data vs $(\varepsilon_{Mh-Mh}/k)^{1/2}$ of these hypothetical molecules M_h with the exception of NO, PH_3, NH_3, and H_2S shows data points lying on the rare gas line. This indicates that the Parmenter et al. correlation is again verified and that the quenching mechanism of the corresponding real quenchers is the same as that of the rare gases. For NO, PH_3, NH_3, and H_2S it has been demonstrated that chemical reactions should play an important role in the removal of $PH_2(\tilde{A}^2A_1)$, and the relative parts of physical and chemical quenchings have been evaluated. It has also been possible to determine the otherwise inaccesible quantity $\varepsilon_{PH_2^*-M}$, i.e., the well depth of the collision complexes, present in the original equation of the Parmenter et al. model. By plotting the quenching data vs $\varepsilon_{PH_2^*-M}/k$, it can be seen again that the Parmenter et al. model is followed by all the quenchers treated, except the above-mentioned molecules.

I. Introduction

In literature a certain number of theoretical models have been reported for the interpretation of the quenching data of excited electronic molecular species due to collisions with other molecules.

An earlier attempt to correlate the quenching efficiencies with some molecular properties of the quenchers has been proposed by Selwyn and Steinfeld[1]

$$\sigma \propto A m_r^{1/2} I_M \alpha_M / r_c^3$$

where σ is the quenching cross section, A a constant, m_r the reduced mass of the collision pair, and I_M and α_M the ionization potential and the polarizability of the quencher, respectively. r_c is the mean distance of closest approach of the collision partners taken to be the hard-sphere distance $(d_P + d_M)/2$, d_P and d_M being the diameters of the excited species and of the quencher, respectively.

Thayer and Yardley's theory[2] is based on the instantaneous dipole−dipole interaction between the excited molecules and the quenchers

$$V = -\sum_{\alpha,\beta} T_{2\alpha\beta} \mu_{\alpha P} \mu_{\beta M} \qquad (1)$$

where the Greek indices refer to the Cartesian coordinates, T_2 is the tensor, and $\mu_{\alpha P}$, $\mu_{\beta M}$ are the electric dipole moment operators for the excited molecule P and for the quencher M, respectively. The interaction operator can induce transitions between the initial and final states of the excited species, and expressions for the transition probabilities have been carried out for nonpolar and polar quenchers.

For nonpolar quenchers, the calculated quenching cross section deduced from the transition probability can be expressed by

$$\sigma = A m_r^{1/2} [I_P I_M/(I_P + I_M)]^2 \alpha_M^2 r_c^{-9} + C \qquad (2)$$

while for polar quenchers it is given by

$$\sigma = A m_r^{1/2} [I_P I_M/(I_P + I_M)]^2 \alpha_M^2 r_c^{-9} + B m_r^{1/2} \mu_M^2 r_c^{-3} + C \qquad (3)$$

where I_P is the ionization potential of P, μ_M the dipole moment of M. A, C, and B are constants deduced from plots of experimental data, the other quantities are defined as above.

The theory of collision complex formation was proposed for the first time in the deactivation of excited electronic states of molecular species by Lee and co-workers in their study of the quenching of $SO_2(\tilde{A}^1A_2)$.[3]

In the collision between the excited species and the quencher, the capture cross section σ_{cap} for the formation of the collision complex is calculated from the effective potential

† Part of the "Vincenzo Aquilanti Festschrift".

* E-mail: Chieu.NguyenXuan@imip.cnr.it. Tel.: +39-0690672217. Fax: +39-0690672238.

10.1021/jp903503z
Published on Web 09/21/2009

$$V(r) = Eb^2/r^2 - C_3/r^3 - C_4/r^4 - C_6/r^6 - C_6'/r^6 \quad (4)$$

where E is the kinetic energy, b the impact parameter, and r the distance between the collision partners. The first term of this expression is the repulsive centrifugal barrier while the other terms represent the attractive multipole interactions (dipole−dipole, dipole−quadrupole, dipole−induced dipole, and dispersion). The coefficients C_n can be found in Table 2 assuming the multipoles in situation of maximum interactions.

σ_{cap} is the maximum quenching cross section at a certain value of E

$$\sigma(E) = P(E)\sigma_{cap}(E) \quad (5)$$

where $\sigma(E)$ and $P(E)$ are the quenching cross section and quenching probability, respectively.

To be compared with experimental quenching data, $\sigma_{cap}(E)$ is thermally averaged.

The procedures for the calculation of $\sigma_{cap}(E)$ and for the thermal averaging operation are described in detail in refs 3, 4, and 5.

Parmenter and co-workers[6,7] have proposed a theory which actually deals with the process of collision-induced de-excitation of excited species in a more general view. It is not restricted to only the phenomenon of excited electronic species quenching but embraces such different processes as collision-induced predissociation, vibrational relaxation, rotational relaxation, vibrational stabilization of a ground state radical.

In this theory, the interaction between the collision partners proceeds via the formation of a collision complex

$$A^* + M \rightarrow [A^* - M] \rightarrow A + M \quad (6)$$

where A* represents the excited species. Further developments of the theory follow two different ways: in one the complex is viewed as a transient pair while in the other it is assumed to be in equilibrium with its separate components, and an equilibrium constant can then be evaluated by well-known formulas involving statistical thermodynamics partition functions. The two treatments lead essentially to the same results, but with the equilibrium assumption of A*−M one obtains a straightforward relationship between the de-excitation cross section and the Lennard-Jones (L-J) potential well depth ε_{A^*-M} of the A*−M complex

$$\ln \sigma = \ln C + \frac{1.67}{T}\frac{\varepsilon_{A^*-M}}{k} \quad (7)$$

where C is a constant, k the Boltzmann constant, and T the temperature.

As ε_{A^*-M} is an unknown quantity, the combining law[8]

$$\varepsilon_{A^*-M} = (\varepsilon_{A^*-A^*}\varepsilon_{M-M})^{1/2} \quad (8)$$

where $\varepsilon_{A^*-A^*}$ and ε_{M-M} are the Lennard-Jones intermolecular well depths for pairs of species A* and pairs of species M molecules, has been used in order to change eq 7 into an equation which relates the quenching cross section to the known ε_{M-M} property of the quenchers. Thus, eq 7 becomes

$$\ln \sigma = \ln C + \beta(\varepsilon_{M-M}/k)^{1/2} \quad (9)$$

where $\beta = 1.67(\varepsilon_{A^*-A^*}/kT^2)^{1/2}$.

These theoretical models have been variously applied in literature to interpret the collision-induced deactivation data of excited electronic states of atomic as well as of molecular species.

In our previous works,[9] we also have employed these theories to attempt a correlation of the quenching data of the $PH_2(\tilde{A}^2A_1; v_2' = 1, 0)$ excited vibronic states with the molecular properties of different quenchers.

The interest of the present work is focused on a new procedure of $PH_2(\tilde{A}^2A_1; v_2' = 1)$ quenching data treatment in the application of the Parmenter et al. model.

TABLE 1: Quenching of $PH_2(\tilde{A}^2A_1; v_2' = 1$ and 0) by Rare Gases, and Diatomic and Polyatomic Molecules[a]

	k_M[b] (10^{-11} cm^3 molecule^{-1} s^{-1})		σ_M[c] (Å^2)	
quencher M	$v_2' = 1$	$v_2' = 0$	$v_2' = 1$	$v_2' = 0$
He	2.51 ± 0.22		1.88 ± 0.17	
Ne	2.03 ± 0.18		2.86 ± 0.25	
Ar	3.24 ± 0.11		5.49 ± 0.18	
Kr	3.78 ± 0.14		7.32 ± 0.27	
Xe	5.50 ± 0.41		11.2 ± 0.8	
H_2	5.79 ± 0.44	2.60 ± 0.10	3.17 ± 0.24	1.42 ± 0.03
N_2	5.05 ± 0.39	2.12 ± 0.10	7.82 ± 0.61	3.28 ± 0.11
CO	7.40 ± 0.62	3.44 ± 0.18	11.5 ± 1.0	5.33 ± 0.27
NO	19.6 ± 1.8	7.70 ± 0.35	30.9 ± 2.9	12.1 ± 0.6
CO_2	8.64 ± 0.43	2.96 ± 0.12	14.9 ± 0.7	5.12 ± 0.21
N_2O	9.07 ± 0.36	2.98 ± 0.11	15.7 ± 0.6	5.16 ± 0.19
H_2S	30.3 ± 2.4	17.2 ± 1.4	49.4 ± 3.9	28.0 ± 2.3
COS	18.4 ± 1.8	8.20 ± 0.34	33.7 ± 3.2	15.1 ± 0.6
SO_2	22.0 ± 2.9		40.9 ± 5.5	
NH_3	34.1 ± 2.1	18.0 ± 1.3	45.4 ± 2.8	24.0 ± 1.8
PH_3	34.4 ± 3.3	24 ± 5	56.0 ± 5.4	39 ± 8
CH_4	5.76 ± 0.33	2.65 ± 0.22	7.53 ± 0.43	3.47 ± 0.29
$CHCl_3$	19.8 ± 1.8	4.98 ± 0.31	40.0 ± 3.7	10.1 ± 0.6

[a] Rate constants k_M, cross sections σ_M. [b] The data are reported with 95% confidence level errors. [c] The cross sections σ_M have been derived from k_M using the formula reported in: Yardley, J. T. *Introduction to Molecular Energy Transfer*; Academic: New York, 1980.

II. Experimental Data of $PH_2(\tilde{A}^2A_1; v_2' = 1, 0)$ Quenching

The quenching rate constants k_M and cross sections σ_M of $PH_2(\tilde{A}^2A_1; v_2' = 1)$ and $PH_2(\tilde{A}^2A_1; v_2' = 0)$ due to different molecules, already reported in ref 9, are presented in Table 1.

A very brief account is here given of the experimental method used to obtain the excited PH_2 electronic state de-excitation data, and the details of which can be found in ref 9 and in references cited therein.

Ground state PH_2 species were generated by photofragmention of PH_3 due to absorption of photons of 193 nm wavelength produced by an ArF excimer laser. Quenching of excited states was studied by the LIF technique. The ground PH_2 radicals were excited by a dye laser to the excited vibronic states under study. The single-exponential time-resolved decay of the fluorescence of these species was then recorded. From a plot of the fluorescence decay constant against the quencher pressure, the quenching constant of the excited PH_2 species due to this quencher can be derived.

Experiments were carried out at room temperature with $T =$ 298 K.

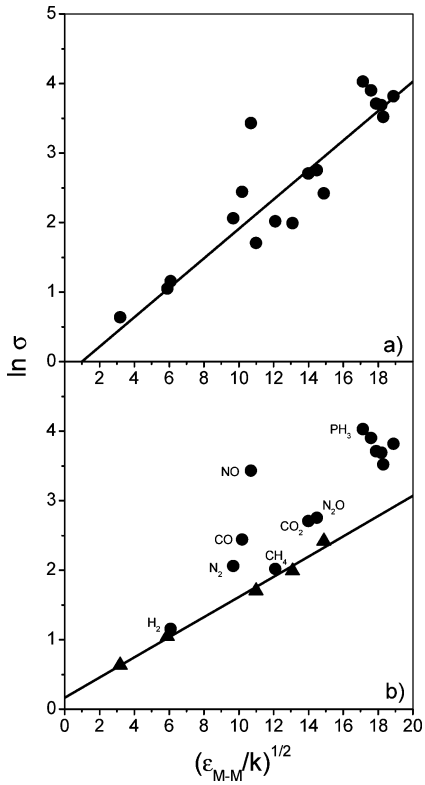

Figure 1. (a) Parmenter et al. plot for $PH_2(\tilde{A}^2A_1; v_2' = 1)$ quenching. Straight line: linear fitting for all data points, except that of NO. (b) Parmenter et al. plot for $PH_2(\tilde{A}^2A_1; v_2' = 1)$ quenching: ▲, rare gas quenchers, He, Ne, Ar, Kr, and Xe; ●, molecular quenchers. Straight line: linear fitting of rare gas data.

III. Correlation of $PH_2(\tilde{A}^2A_1; v_2' = 1, 0)$ Quenching with Molecular Properties of the Quenchers. Parmenter and Co-workers' Equation

In the previous paper,[9] we have seen that none of the last three models presented in the Introduction section leads to a satisfatory correlation of the quenching data of the PH_2 excited electronic species.

With the Thayer and Yardley's and Lee et al. models, there is not much else to do if not noting their inability in establishing for all the quenchers considered, rare gases and molecular quenchers, the same correlation.

With the Parmenter et al. model the situation is different, and we are going to analyze it in detail.

The first thing we notice in this model is the simplicity of the equation which relates the deactivation cross section to the quencher properties represented here only by the well depth ε_{M-M}.

In Figure 1a, we plot the quenching data of $PH_2(\tilde{A}^2A_1; v_2' = 1)$ against $(\varepsilon_{M-M}/k)^{1/2}$ (the different ε_{M-M}/k are reported below in Table 3). If NO is not taken into account, the data on the whole seem to follow the theory, at least for what concerning the approximate variation trend of the quenching efficiency with respect to the variation of the well depth ε_{M-M} of the quencher. Data linear fitting is represented by the straight line.

Rare gases have been the first quenchers to be studied, and we have seen that they obey the Parmenter et al. equation very closely. This fact with rare gases has been seen to occur with the quenching of other systems, one of which is propynal $1A''$ for which the theory of Thayer and Yardley has been worked out.[2] Then came experiments with diatomic quenchers and successively with the polyatomic ones.

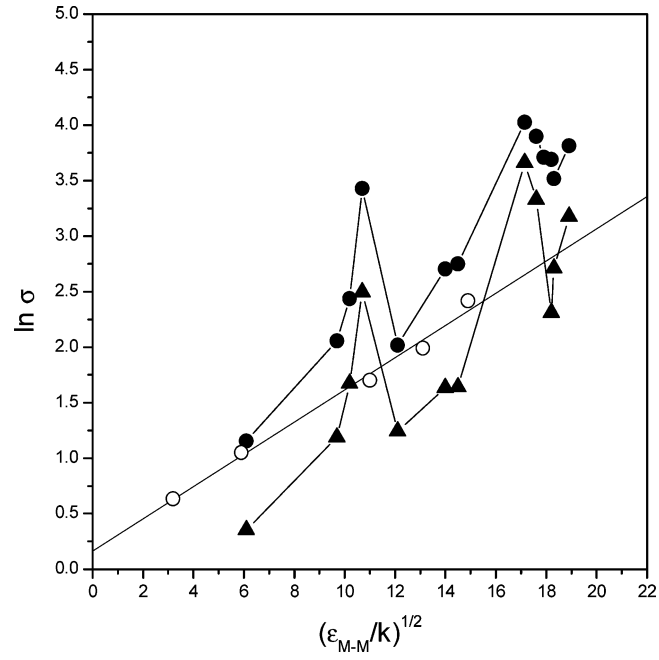

Figure 2. Parmenter et al. plots for $PH_2(\tilde{A}^2A_1; v_2' = 1)$ and $PH_2(\tilde{A}^2A_1; v_2' = 0)$ quenching: ●, $v_2' = 1$ quenching by molecular quenchers; ○, $v_2' = 1$ quenching by rare gas quenchers. Straight line: linear fitting of rare gas data. ▲, $v_2' = 0$ quenching by molecular quenchers.

As can be seen in Figure 1b, the data of the molecular quenchers deviate from the variation trend displayed by rare gases.

It is this way of considering quenchers with successively higher complexities that has permitted us to be aware of the existence of difference in deactivation trend between rare gases and the other molecules.

This has induced us not to consider rare gases and the molecular quenchers as a homogeneous group in the quenching of $PH_2(\tilde{A}^2A_1)$ as it has been done in Figure 1a by performing the linear fitting of all the quenchers, except NO, together.

In the quenching studies of $PH_2(\tilde{A}^2A_1)$, two independent series of measurements have been carried out, one for the bending mode $v_2' = 1$ and the other for $v_2' = 0$. The queching data of these two vibrational species are plotted in the same Figure 2.

The striking feature observed in these plots is their parallelism, which shows that the differences of quenching data between the different quenchers reflect faithfully the effective differences in efficiency of these molecules in deactivating the excited PH_2 species. Thus the increase of the quenching cross sections going from H_2 to NO passing by N_2 and CO, and then their decrease in CH_4, and again increase to CO_2, N_2O, PH_3 followed by the series of decreases for the rest of the quenchers studied, are real. The same can be said of the difference between the variation trend of these molecules and that of rare gas quenchers.

All these facts induce a more accurate examination of these data in relation to the Parmenter et al. theory in order to possibly obtain an insight into the origin of these differences that the different ε_{M-M} values by themselves cannot explain.

In our previous works,[9] a certain number of attempts have been made to cope with this problem, but none of these has given rise to a satisfactory solution.

One of the very first problems we had to face was to produce an explanation for the observed trend of increasing quenching efficiency from H_2 to NO for diatomic quenchers. The higher cross sections of N_2, CO, and NO with respect to the values deduced from the rare gas line at the respective values of $(\varepsilon_{M-M}/$

$k)^{1/2}$ must be due to some additional deactivation channels which in the case of NO can easily be ascribed to chemical reactivity as chemical reactions between NO and ground electronic states $PH_2(\tilde{X}^2B_1;\ v_2'' = 0)$ and $PH_2(\tilde{X}^2B_1;\ v_2'' = 1)$ have been seen to occur and the constants of which have been measured.[10]

As the vibration frequencies of H_2, N_2, CO, and NO are 4401, 2359, 2170, and 1904 cm^{-1}, respectively, another type of additional channel could be an intermolecular V−V energy transfer between these molecules and $PH_2(\tilde{A}^2A_1;\ v_2' = 1)$, with this latter deactivated to $v_2' = 0$

$$PH_2(\tilde{A}^2A_1;v_2' = 1) + M(v = 0) \rightarrow PH_2(\tilde{A}^2A_1;v_2' = 0) + M(v = 1) \quad \Delta E$$

producing the observed increasing trend which corresponds to a decreasing ΔE energy gap between the quencher and $v_2' = 1$. This process, however, cannot be considered as the same trend is observed for $PH_2(\tilde{A}^2A_1;\ v_2' = 0)$.

The intermolecular $E-V$ process has also been contemplated with the excited species deactivated to some vibrational level of the ground electronic state, and the energy difference, equal to the vibrational frequency of the quencher, transferred to this latter

$$PH_2(\tilde{A}^2A_1;v_2' = 1,0) + M(v = 0) \rightarrow PH_2(\tilde{X}^2B_1;v'') + M(v = 1)$$

$\Delta E[(v_2' = 1,\ 0) - v_2''] = \Delta E[M(v = 1) - M(v = 0)]$. The lower the quencher frequency is, the higher the energy transfer efficiency should be, and this should account for the observed quenching trend of diatomic molecules. However, the data of CH_4, which has two normal vibrational frequencies much lower than those of N_2 and CO, contradict this mechanism.

Experiments were carried out to probe possible occurrence of chemical reactions between ground-state $PH_2(\tilde{X}^2A_1;\ v_2'' = 0)$ and all the quenchers studied. The result was that none of these molecules, except NO, gave rise to reaction, confirming the endothermicity found in the thermochemical calculations made for their possible reactive processes. With $PH_2(\tilde{A}^2A_1;\ v_2' = 1, 0)$, by taking into account the electronic energy, these latter turn exothermic and from the energetic point of view they would become possible. This is the case for reactions such as

$$PH_2(\tilde{A}^2A_1;v_2' = 1,0) + H_2 \rightarrow PH_3 + H$$

$$PH_2(\tilde{A}^2A_1;v_2' = 1,0) + CH_4 \rightarrow PH_3 + CH_3$$

However, from Figure 1b, it can be seen that no reaction has taken place between these quenchers and $PH_2(\tilde{A}^2A_1)$. H_2 and CH_4 behave like rare gases. Thus, in the case of excited electronic species, the energetic factor is not a sufficient condition for the occurrence of a reaction, and, except for NO, proposing chemical reactions as additional de-excitation channels of $PH_2(\tilde{A}^2A_1;\ v_2' = 1,\ 0)$ for all the other molecular quenchers does not seem, without further evidence, to have a sound basis.

If all the mentioned mechanisms do not give a satisfactory interpretation of the observed different behavior of the molecular quenchers with respect to that of the rare gases, and as these differences exist, we have intuitively to ascribe them to differences in molecular properties such as multipole potentials which should, for instance, generate more or less tight collision complexes giving rise to different quenching efficiencies. This is at most only a qualitative consideration, but what we need is something more quantitative which could justify the observed phenomena.

The main purpose of the present work is to rationalize the differences between molecular quenchers and rare gases in the deactivation of $PH_2(\tilde{A}^2A_1)$ on a quantitative basis.

If temporarily we can leave apart the chemical reactions and consider the quenching of excited PH_2 electronic species as due only to physical processes, then it becomes clear that the differences between molecular quenchers and rare gases must derive from the fact that these latter are provided with polarizabilities as the only electric properties while the electric behavior of the molecular quenchers is determined also by dipole and quadrupole moments. This idea seems to be confirmed by CH_4 which, being provided only with polarizability, behaves like a rare gas.

1. Real Quenchers and Equivalent Rare Gas-like Molecules. If the $PH_2(\tilde{A}^2A_1)$ de-excitation mechanisms of molecular quenchers are the same as those due to rare gases, it should be possible to think of hypothetical rare gas-like molecules provided with only polarizability, indicated here as α_{Mh}, and having quenching efficiencies equal to efficiencies of the real quenchers.

According to eq 7, the efficiency determining quantity is the $\varepsilon_{PH_2^*-M}$ well depth of the collision complex PH_2^*-M, with PH_2^* representing $PH_2(\tilde{A}^2A_1)$. Therefore, the mentioned hypothetical molecule, which we designate by M_h, should form a collision complex $PH_2^*-M_h$ which must have a well depth equal to that of PH_2^*-M.

The principle that we propose for the determination the polarizability of the hypothetical molecule is based on (a) the construction of a Lennard-Jones type potential for the collision complex PH_2^*-M of the real quencher M, (b) the construction of a Lennard-Jones type potential containing the polarizability α_{Mh} as parameter for the collision complex $PH_2^*-M_h$, (c) calculation of the well depth of (a) and of the well depth of (b), and (d) determination of the polarizabilty α_{Mh} of M_h, by setting equal the two well depths found in (c).

Clearly the well depth of (a) cannot be considered as the true well depth of the PH_2^*-M complex potential, it is used here only as a reference value for the determination of the characteristics of the equivalent M_h molecule.

The Lennard-Jones type potential between PH_2^* and a real quencher M should be expressed by

$$V_M(r) = \frac{d_M}{r^{12}} - \frac{C_{M,n}}{r^n} \tag{10}$$

d_M/r^{12} is the repulsive term, while $C_{M,n}/r^n$ stands for the attractive one.

$C_{M,n}/r^n$ actually represents a sum of attractive multipole interactions between PH_2^* and M: dipole−dipole, dipole−quadrupole, dipole−induced dipole, and dispersion. The different terms are shown in Table 2.

A similar expression has been used in the effective interaction potential eq 4 of the above-mentioned collision complex formation model[3] for the calculation of the capture cross section σ_{cap}.

All the multipole interaction terms are normally dependent on the orientations of the interacting molecules, and the global

TABLE 2: Different Multipole Interaction Terms of $C_{M,n}/r^n$

interaction	orientation angle average[a,c]	maximum interaction[a,b,c]
dipole−dipole	$\frac{2}{3kT}\frac{\mu_P^2\mu_M^2}{r^6}$	$\frac{2\mu_P\mu_M}{r^3}$
dipole−quadrupole	$\frac{1}{kT}\left(\frac{\mu_P^2Q_M^2+\mu_M^2Q_P^2}{r^8}\right)$	$\frac{3}{2}\left(\frac{\mu_PQ_M+\mu_MQ_P}{r^4}\right)$
dipole−induced dipole	$\frac{\mu_P^2\alpha_M+\mu_M^2\alpha_P}{r^6}$	$\frac{2(\mu_P^2\alpha_M+\mu_M^2\alpha_P)}{r^6}$
dispersion	$\frac{3}{2}\frac{I_PI_M}{I_P+I_M}\frac{\alpha_P\alpha_M}{r^6}$	$\frac{3}{2}\frac{I_PI_M}{I_P+I_M}\frac{\alpha_P\alpha_M}{r^6}$

[a] Reference 8. [b] References 3, 4, and. 5. [c] P stands for PH_2*. μ, Q, α, and I are dipole moment, quadrupole moment, polarizability, and ionization potential, respectively.

interaction can be obtained by carrying out an averaging operation over all orientations of the two molecules.

In Table 2, the different $C_{M,n}/r^n$ terms are reported for the angle averaged potentials and also for the case of most favorable mutual orientations and maximum interations.

In the following, both cases will be discussed.

The d_M parameter of eq 10 is determined by setting $V_M(r) = 0$ when r is equal to the hard sphere closest distances between the collision partners, r_{cM}.

Quantitative calculations can be carried out using the molecular properties shown in Table 3.

The published data of these properties often present discrepancies which sometimes can be quite large especially for the quadrupole moments. These discrepancies are usually due to different experimental methods employed for the determination of these quantities.

For the PH_2* radical, no data are available in literature, and those reported in Table 3 are estimated values based on calculations.

The diameter of PH_2 is assumed to be approximately equal to that of H_2S.

The dipole moment has been calculated using the method outlined by Smyth[11] and the P−H bond moment reported in his book

$$\mu = (m_1^2 + m_2^2 + 2m_1m_2\cos\theta)^{1/2}$$

where m_1 and m_2 are the two P−H bond moments and θ is the HPH angle. P−H bond moment is 0.36 D. The HPH angle of 123.0° for $PH_2(\tilde{A}^2A_1)$ is that given by Herzberg.[12]

The method proposed by Eubank[13] for estimation of quadrupole moments has been here adopted. As PH_2 is a noncylindrically symmetric molecule, the effective molecular quadrupole moment can be obtained from the empirical equation

$$Q^2 = (2/3)(Q_{xx}^2 + Q_{yy}^2 + Q_{zz}^2)$$

By calculating the diagonal elements Q_{ii} with the bond dipole method reported by Eubank, Q can be derived and its value is shown in Table 3.

Additivity of bond polarizabities has been applied to calculate polarizability of PH_2 from that of PH_3.

The ionization potential of $PH_2(\tilde{A}^2A_1;\ v_2' = 1)$ has been deduced from that of $PH_2(\tilde{A}^2A_1;\ v_2' = 0)$ reported in ref 9.

To our knowledge, for the excited electronic species $PH_2(\tilde{A}^2A_1)$, the angle HPH and the distance P−H of 1.435 Å[12] are the only quantities, connected with the molecular electric properties, available from literature, so the reported values of these properties in Table 3 for this radical are the best ones that we have been able to estimate with our calculations.

For cylindrically symmetric $CHCl_3$, Q_{zz} has been calculated by the same above-mentioned bond dipole method.

The values of the different properties of Table 3 have been selected from literature data on the basis of consistency of results between different quenchers, and happen to correspond often to those adopted by other authors.

The well depth of the potential function eq 10, designated by $(V_M)_{min}$, can then be determined by plotting the function or analytically.

2. Determination of the Hypothetical Polarizabilities α_{Mh}. The Lennard-Jones type potential function for the hypothetical rare gas-like quencher which should have only polarizability as electric property and no dipole nor quadrupole, and which should form with the PH_2 excited species a collision complex having a well depth equal to that due to the actual quencher should be expressed by

$$V_{Mh}(r) = \frac{d_{Mh}}{r^{12}} - \frac{C_{Mh,6}}{r^6} - \frac{C'_{Mh,6}}{r^6} \qquad (11)$$

$C_{Mh,6}$ and $C'_{Mh,6}$ are coefficients for dipole−induced dipole and dispersion interactions, respectively. They are given in Table 2, and as can be seen $C_{Mh,6}$ for maximum interaction is twice that of orientation angle averaged potential.

TABLE 3: Selected Molecular Properties of PH_2 and the Investigated Quenchers: Diameter (d_M), Dipole Moment (μ_M), Quadrupole Moment (Q_M), Polarizability (α_M), Ionization Potential (I_M), Potential Well Depth (ε_{M-M}/k)

PH_2 and quenchers M	d_M[a] (Å)	μ_M[c] (debye)	Q_M[e] (Å^2)	α_M[e] (Å^3)	I_M[e] (eV)	ε_{M-M}/k[f] (K)
PH_2	3.591[b]	0.3435[d]	0.153[d]	2.85[d]	7.439[d]	
He	2.6	0	0	0.204	24.6	10.2
Ne	2.8	0	0	0.393	21.6	34.8
Ar	3.4	0	0	1.66	15.7	121.0
Kr	3.6	0	0	2.48	14.0	171.6
Xe	4.1	0	0	4.00	12.1	222.0
H_2	3.0	0	0.14	0.79	15.4	37.2
N_2	3.7	0	0.316	1.76	15.6	94.1
CO	3.6	0.112	0.52	1.95	14.0	104.0
NO	3.5	0.153	0.374	1.74	9.25	114.5
CO_2	4.00	0	0.897	2.65	13.77	196.0
N_2O	3.879	0.167	0.91	3.03	12.89	210.3
H_2S	3.591	0.97	0.584	3.78	10.453	309
COS	4.13	0.712	0.183	5.7	11.1	334.9
SO_2	4.29	1.63	0.92	3.78	12.3	320.4
NH_3	3.15	1.47	0.707	2.26	10.19	357.2
PH_3	3.5	0.58	0.478	4.27	9.87	294[g]
CH_4	3.80	0	0	2.6	12.71	146.4
$CHCl_3$	5.430	1.01	1.017	8.23	11.4	331.2

[a] Data mostly from Chan, S. C.; Rabinovitch, B. S.; Bryant, J. T.; Spicer, L. D.; Fujimoto, T.; Lin, Y. N.; Pavlou, S. P. *J. Phys. Chem.* **1970**, *74*, 3160, and from ref 8. [b] As the diameter of PH_2 is unknown, we have adopted for it the diameter of H_2S. [c] Nelson, R. D., Jr.; Lide, D. R., Jr.; Maryott, A. A. *Selected Values of Electric Dipole Moments for Molecules in the Gas phase;* NSRDS-NBS10; National Standard Reference Data Series, National Bureau of Standards 10; National Bureau of Standards: U.S. Department of Commerce, 1967. [d] Calculated values (see Text). [e] The values of Q_M, α_M, and I_M are selected from the following papers: Reference 2. Reference 3. Reference 4. Reference 5. Reference 8. Maryott, A. A.; Buckley, F. *Natl. Bur. Stand. (U.S.), Circ. 537* **1953**. Stogryn, D. E.; Stogryn, A. P. *Mol. Phys.* **1966**, *11*, 371. Lippincott, E. R.; Nagarajan, G.; Stutman, J. M. *J. Phys. Chem.* **1966**, *70*, 78. Flygare, W. H.; Benson, R. C. *Mol. Phys.* **1971**, *20*, 225. Radzig, A. A.; Smirnov, B. M. *Reference Data on Atoms, Molecules, and Ions*; Springer: Berlin, 1985. Combariza, J.; Salzman, W. R.; Kukolich, S. G. *Chem. Phys. Lett.* **1990**, *167*, 607. Phillips, L. F. *Chem. Phys. Lett.* **1990**, *165*, 545. Benzi, P.; Operti, L.; Rabezzana, R.; Splendore, M.; Volpe, P. *Int. J. Mass Spectrom. Ion Processes* **1996**, *152*, 61. García-Moreno, I.; Figuera, J. M.; Castillejo, M.; Rodríguez, J. C. *J. Phys. Chem.* **1993**, *97*, 8414. Khristenko, S. V.; Maslov, A. I.; Shelveko, V. P. *Molecules and Their Spectroscopic Properties*; Springer: Berlin, 1998. van Duijnen, P. T.; Swart, M. *J. Phys. Chem. A* **1998**, *102*, 2399. Doerksen, R. J.; Thakkar, A. J.; Koga, T.; Hayashi, M. *J. Mol. Struct. (THEOCHEM)* **1999**, *488*, 217. Couling, V. W.; Graham, C. *Mol. Phys.* **2000**, *98*, 135. Noorizadeh, S.; Parhizgar, M. *J. Mol. Struct. (THEOCHEM)* **2005**, *725*, 23. [f] Reference 6. [g] Estimated value: Nguyen Xuan, C.; Margani, A. *J. Chem. Phys.* **1998**, *109*, 9417.

The other properties of the hypothetical quencher such as diameter, mass and ionization potential are those of the corresponding real quencher.

Equation 11 has two parameters to be determined, one is d_{Mh} and the other is α_{Mh} itself.

We first find the minimum of $V_{Mh}(r)$ by setting equal to zero its derivative with respect to r. The following equation is obtained

$$r^{-6} = \frac{C_{Mh,6} + C'_{Mh,6}}{2d_{Mh}} \tag{12}$$

By defining

$$C_{Mh,6} = U_{Mh}\alpha_{Mh}$$

and

$$C'_{Mh,6} = W_{Mh}\alpha_{Mh}$$

eq 12 becomes

$$r^{-6} = \frac{U_{Mh} + W_{Mh}}{2d_{Mh}}\alpha_{Mh} \tag{13}$$

U_{Mh} and W_{Mh} can be deduced from Table 2.

Substitution of eq 13 into eq 11 gives the $V_{Mh}(r)$ well depth, which has to be equal, as said above, to $(V_M)_{min}$. We then obtain

$$\frac{(U_{Mh} + W_{Mh})^2\alpha_{Mh}^2}{4d_{Mh}} = -(V_M)_{min} \tag{14}$$

The minus sign is due to the fact that the minimum of potential eq 10 as well as that of eq 11 have negative values.

The second equation relating d_{Mh} to α_{Mh} is obtained by imposing $V_{Mh}(r) = 0$ when r is equal to hard sphere closest distances between the collision partners, r_{cM}

$$d_{Mh} = \frac{\alpha_{Mh}(U_{Mh} + W_{Mh})}{r_{cM}^{-6}} \tag{15}$$

By combining the two eqs 14 and 15, d_{Mh} and α_{Mh} can be derived.

Table 4 reports the values of α_{Mh} for both cases of maximum and orientation averaged interactions.

3. Conversion of α_{Mh} of the Rare Gas-like Hypothetical Quenchers in ε_{Mh-Mh}/k. ε_{Mh-Mh}/k is the well depth of the potential of a pair of hypothetical molecules, corresponding to ε_{M-M}/k of the equivalent real quencher.

By plotting in Figure 3 the ε_{M-M}/k values reported in Table 3 against the polarizabilities α_M of the rare gas series He, Ne, Ar, Kr, and Xe, we have seen that a linear dependence exists between these two quantities. CH_4 is seen to behave in the same way having polarizability as sole molecular electric property.

The linear regression fitting of the rare gas data gives the following expression

$$\varepsilon_{M-M}/k = (56.16 \times \alpha_M) + 13.79 \tag{16}$$

As the hypothetical quenchers are presumed to have rare gas characteristics, it is reasonable to use eq 16 to derive their ε_{Mh-Mh}/k values from the calculated α_{Mh}.

In Figure 3 we have also plotted the data of COS. As can be seen, COS also lies on the rare gas line even if this molecule possesses, besides polarizability, also dipole and quadrupole moments. As its polarizability is high, and as dispersion usually predominates over the other multipole interactions, the quantity ε_{M-M}/k of COS seems to be essentially determined by the polarizability of the molecule like what happens with the rare gases.

TABLE 4: ε_{M-M}/k, and Calculated α_{Mh} and ε_{Mh-Mh}/k of Molecular Quenchers for Both Orientation Angle Averaged and Maximum Multipole Interactions Used in L-J Type Potential Attractive Branch

		orientation angle averaging		maximum interaction	
quenchers M	ε_{M-M}/k^a (K)	α_{Mh} (Å^3)	ε_{Mh-Mh}/k (K)	α_{Mh} (Å^3)	ε_{Mh-Mh}/k (K)
H_2	37.2	0.792	58.3	0.956	67.5
N_2	94.1	1.77	113.1	2.22	138.2
CO	104.0	1.98	124.8	2.98	181.1
NO	114.5	1.76	112.6	2.79	170.2
CO_2	196.0	2.72	166.3	4.12	244.9
N_2O	210.3	3.11	188.2	4.97	292.8
H_2S	309	3.98	237.5	7.52	435.9
COS	334.9	5.79	339.0	8.40	485.4
SO_2	320.4	4.29	254.4	11.27	646.7
NH_3	357.2	2.72	166.3	7.07	411.1
PH_3	294	4.36	258.4	6.65	387.2
CH_4	146.4	2.60	159.8	2.60	159.8
$CHCl_3$	331.2	8.46	489.1	15.85	903.8

[a] Literature data: ref 6.

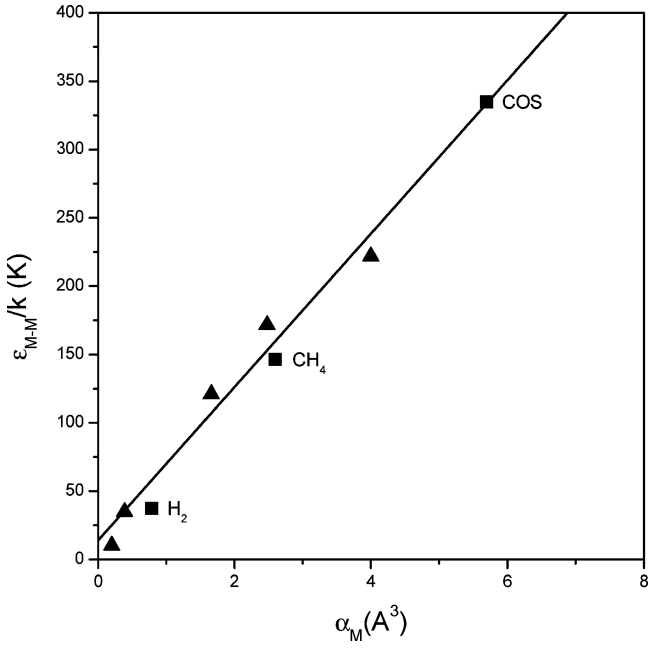

Figure 3. Plot of ε_{M-M}/k vs polarizability α_M of rare gases (▲) and some molecules (■). Straight line: linear fitting with rare gas data.

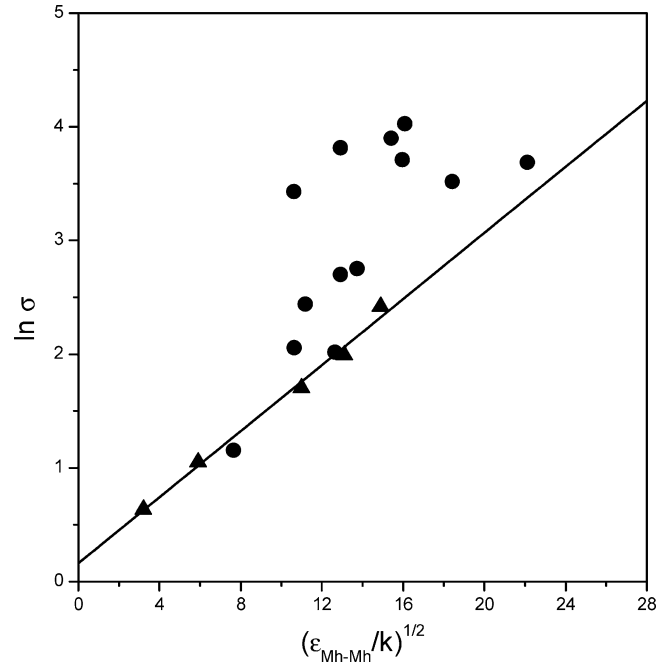

Figure 4. $PH_2(\tilde{A}^2A_1;\ v_2' = 1)$ quenching: ●, ln σ vs $(\varepsilon_{Mh-Mh}/k)^{1/2}$ calculated with orientation angle averaged multipole interactions (see text) for molecular quenchers; ▲, ln σ vs $(\varepsilon_{M-M}/k)^{1/2}$, literature data shown in Table 3 for rare gases. Straight line: linear fitting of rare gas data.

Table 4 displays the different ε_{Mh-Mh}/k values calculated for both angle averaged and maximum multipole interactions.

4. ln σ vs $(\varepsilon_{Mh-Mh}/k)^{1/2}$ Plot and Resulting Observations. As rare gas-like M_h is equivalent to M, we can plot ln σ vs $(\varepsilon_{Mh-Mh}/k)^{1/2}$ according to the Parmenter et al. eq 9.

Figures 4 and 5 display this plot with ε_{Mh-Mh}/k derived from angle averaged interactions and from maximum interactions of the multipoles, respectively. For rare gases the abscissae are given by ε_{M-M}/k of Table 3.

By using the angle averaged multipole interactions in the building of the attractive branch of the Lennard-Jones type potentials, the relationship between the quenching cross sections and the calculated ε_{Mh-Mh}/k values, as shown by Figure 4, does not improve with respect to Figure 1b, on the contrary it becomes worse as the data scattering spreads over a larger area of the plot.

Figure 5, obtained with the ε_{Mh-Mh}/k values calculated from potentials in which the attraction of the collision partners is governed by maximum multipole interactions as expressed in Table 2, conversely, shows a much better situation. With the exception of NO, PH_3, NH_3, and H_2S, the data points are seen to move on the rare gas line confirming the validity of the Parmenter et al. Equation 9.

As can be seen, the results shown in Figure 5 have been achieved with ε_{Mh-Mh}/k deduced, through the rare gas plot ε_{M-M}/k vs α_M of Figure 3, from the polarizabilities α_{Mh} determined by pure mathematical operations on electric multipole data of the real quenchers and PH_2*.

The fact that, by plotting the experimental quenching data of the real quenchers against these ε_{Mh-Mh}/k calculated values, we obtain points which agree very well with the points of the rare gas line at the same ε_{Mh-Mh}/k values demonstrates that the real quenchers dealt with, with the exception of the few molecules already mentioned above, i.e., NO, PH_3, NH_3, and H_2S, behave really as rare gases for what concerning the de-excitation process of $PH_2(\tilde{A}^2A_1)$. In other words, the quenching mechanism due to these molecules is only of physical nature and consists in inducing the transition of the PH_2 radical from the excited $(\tilde{A}^2A_1;\ v_2' = 1)$ state to the underlying isoenergetic

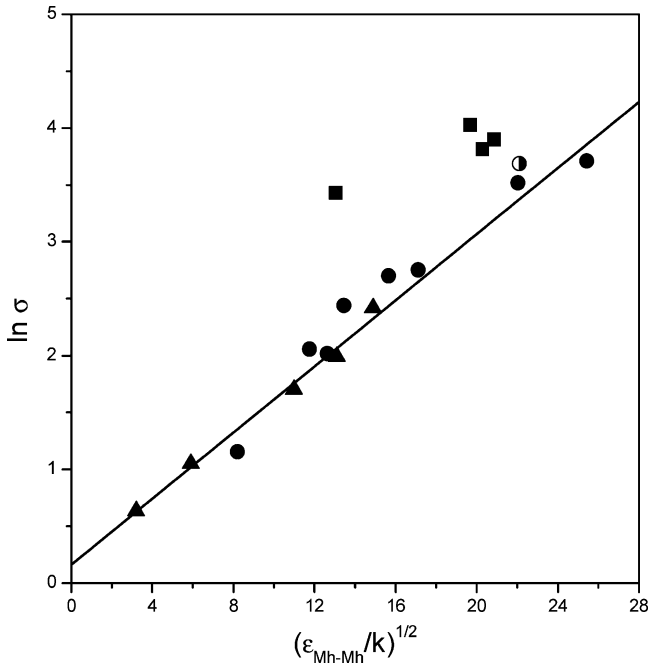

Figure 5. $PH_2(\tilde{A}^2A_1;\ v_2' = 1)$ quenching: ●, ln σ vs $(\varepsilon_{Mh-Mh}/k)^{1/2}$ calculated in conditions of maximum multipole interactions for H_2, CH_4, N_2, CO, CO_2, N_2O, COS, and SO_2; ◑, ln σ vs $(\varepsilon_{Mh-Mh}/k)^{1/2}$ calculated with orientation angle averaged multipole interactions for $CHCl_3$; ■, ln σ vs $(\varepsilon_{Mh-Mh}/k)^{1/2}$ calculated in conditions of maximum multipole interactions for NO, PH_3, NH_3, and H_2S; ▲, ln σ vs $(\varepsilon_{M-M}/k)^{1/2}$, literature data shown in Table 3 for rare gases. Straight line: linear fitting of rare gas data.

TABLE 5: Experimental $PH_2(\tilde{A}^2A_1;\ v_2' = 1)$ Quenching Cross Section σ_{exp}, $(\varepsilon_{Mh-Mh}/k)^{1/2}$,[a] σ_{calc},[b] σ_{chem},[c] $\sigma_{chem}/\sigma_{phys}$ of the Quenchers That Do Not follow the Parmenter et al. Correlation

Quenchers	σ_{exp} (Å^2)	$(\varepsilon_{Mh-Mh}/k)^{1/2}$	$\sigma_{calc} = \sigma_{phys}$ (Å^2)	σ_{chem} (Å^2)	$\sigma_{chem}/\sigma_{phys}$
NO	30.9	13.05	7.80	23.1	3.0
PH_3	56.0	19.68	20.4	35.6	1.7
NH_3	45.4	20.28	22.3	23.1	1.0
H_2S	49.4	20.88	24.3	25.1	1.0

[a] Data obtained from maximum multipole interaction calculations. [b] Calculated cross section from the rare gas line of Figure 5 using the $(\varepsilon_{Mh-Mh}/k)^{1/2}$ values. σ_{calc} can be considered as due to physical quenching, i.e., σ_{phys}. [c] Presumed chemical part of the total quenching cross section: $\sigma_{chem} = \sigma_{exp} - \sigma_{calc}$.

higher vibrational levels of the ground electronic state $PH_2(\tilde{X}^2B_1)$.[14]

Besides, the fact that the quantities ε_{Mh-Mh}/k deduced from pure mathematical operations lead to rare gaslike M_h molecules, equivalent of real quenchers, which behave as the real rare gases constitutes the proof that the whole procedure for their determination, starting from the construction of the Lennard-Jones type potentials for the complexes PH_2*−M and PH_2*−M_h, is correct.

We have thus also shown that for most molecular quenchers the physical quenching process is the result of combining effects of polarizability, dipole, and quadrupole moments.

A special attention has to be drawn to the data point of $CHCl_3$ in Figure 5, which has been obtained from Lennard-Jones type potentials with attractive branches built not by maximum multipole interactions like for the other quenchers but instead by angle averaged interactions. As shown in Table 4, calculations by maximum interactions of the multipoles give to this quencher a too large value for the calculated ε_{Mh-Mh}/k.

The peculiar situation of $CHCl_3$ will be dealt with later on.

Figures 4 and 5 give us another important piece of information concerning the way the collision partners approach one another. For all the quenchers studied, except $CHCl_3$, PH_2* and the quenching molecule come together in orientation angles suitable for most favorable interactions.

What also comes out clearly from Figure 5 is the different nature of the processes involved by NO, PH_3, NH_3, and H_2S in the deactivation of the PH_2 excited electronic species. If the removal of these latter is not due exclusively to chemical reactions with those molecules, Figure 5 would allow to determine the respective amounts of physical and chemical contributions to the global cross sections. In fact, from the rare gas line represented by

$$\ln \sigma = 0.145(\varepsilon_{M-M}/k)^{1/2} + 0.162$$

the quenching cross section parts due to pure collisional interactions can be calculated. The chemical quenching cross sections are derived from differences between the total cross sections and these latter calculated quantities.

At the beginning of section III, we have said that for lack of concrete evidence we cannot ascribe the differences between the quenching cross sections of molecular quenchers and the values deduced from the rare gas trend to additional quenching channels due to chemical reactions. Figure 5 now can produce this evidence for NO, PH_3, NH_3, and H_2S.

Table 5 reports the physical and chemical parts of the quenching efficiencies of these molecules.

In a previous paper,[10] we have listed a certain number of possible reactions of NO with PH_2. With ground $PH_2(\tilde{X}^2A_1)$ all the reactions considered except

$$PH_2 + NO \rightarrow PN + H_2O \qquad (17)$$

$$\Delta H = (-95.9) - (-83.7)\ \text{kcal mol}^{-1}$$

are endothermic. Therefore, the above reaction of PH_2 with NO giving rise to the formation PN and H_2O is highly probable. With excited $PH_2(\tilde{A}^2A_1;\ v_2' = 1, 0)$ having vibronic energy contents of 55.0 and 52.3 kcal/mol for $v_2' = 1$ and $v_2' = 0$, respectively, the thermochemical situation changes. Apart from the above reaction which becomes even more exothermic with excited PH_2, some of the endothermic reactions such as

$$\begin{aligned} PH_2 + NO &\rightarrow PNH + OH \\ &\rightarrow HPN + OH \\ &\rightarrow PN + H + OH \\ &\rightarrow HPNH + O \\ &\rightarrow HNO + PH \\ &\rightarrow HPO + NH \end{aligned}$$

now turn exothermic and could from the energetic point of view contribute to the removal of $PH_2(\tilde{A}^2A_1;\ v_2' = 1, 0)$. However, reaction 17 as having the highest exothermicity should be predominant.

TABLE 6: Quenching of $PH_2(\tilde{A}^2A_1; v_2' = 1)$, Calculated Well Depth $\varepsilon_{PH_2^*-M}/k$ of the Collision Complex PH_2^*-M

quenchers	ε_{Mh-Mh}/k (K)[a]	$\varepsilon_{PH_2^*-M}/k$ (K)[b]	quenchers	ε_{Mh-Mh}/k (K)	$\varepsilon_{PH_2^*-M}/k$ (K)
He		82.9	CO_2	244.9	406.0
Ne		153.0	N_2O	292.8	444.0
Ar		285.4	H_2S	435.9	541.7
Kr		339.8	COS	485.4	571.6
Xe		386.5	SO_2	646.7	659.7
H_2	67.5	213.1	NH_3	411.1	526.0
N_2	138.2	305.0	PH_3	387.2	510.5
CO	181.1	349.1	CH_4	159.8	328.0
NO	170.2	338.5	$CHCl_3$	489.1[c]	573.7

[a] Data obtained from maximum multipole interaction calculations. [b] For M = rare gases, we have calculated $\varepsilon_{PH_2^*-M}/k$ using the literature data ε_{M-M}/k of Table 3. [c] Data obtained from orientation angle averaged multipole interaction calculations.

For PH_3, NH_3, and H_2S, metathesis reactions

$$PH_2^* + PH_3 \rightarrow PH_3 + PH_2$$

$$PH_2^* + NH_3 \rightarrow PH_3 + NH_2$$

$$PH_2^* + H_2S \rightarrow PH_3 + HS$$

should be the most probable ones.

From the above discussion, it becomes clear that the Parmenter et al. eq 9 is strictly verified only by rare gas quenchers and not by most of the other molecules. This should be due to the fact that the combining rule, relating the well depth of the PH_2^*-M complex to the well depths $\varepsilon_{PH_2^*-PH_2^*}$ and ε_{M-M} considered separately, and from which eq 9 is derived, is not valid for most of the molecular quenchers. In effect, when the calculated $(\varepsilon_{Mh-Mh}/k)^{1/2}$ quantities of the rare gas-like simulation entities are used for the Parmenter et al. plot, the data points, with the exception of NO, PH_3, NH_3, and H_2S, thus obtained agree quite well with the rare gas line as shown in Figure 5. This indicates that eq 9 resumes working when the $(\varepsilon_{Mh-Mh}/k)^{1/2}$ values of the rare gas-like molecules, for which the combining rule is valid, are used instead of the $(\varepsilon_{M-M}/k)^{1/2}$ values of the real quenchers.

From Figure 5, and using only the rare gas data which follow closely the Parmenter et al. eq 9, the slope β and then $\varepsilon_{PH_2^*-PH_2^*}/k$ can be derived. $\varepsilon_{PH_2^*-PH_2^*}/k$ results to be 673.1 K corresponding to a value of 1.34 kcal/mol for $\varepsilon_{PH_2^*-PH_2^*}$.

Using the different calculated values of ε_{Mh-Mh}/k for maximum multipole interactions between PH_2^* and the quenchers of Table 4 in combination with this value of $\varepsilon_{PH_2^*-PH_2^*}/k$, we calculate according the combining rule

$$\frac{\varepsilon_{A-M}}{k} = \sqrt{\frac{\varepsilon_{A-A}}{k}\frac{\varepsilon_{M-M}}{k}}$$

the different quantities $\varepsilon_{PH_2^*-Mh}/k$. As M_h has the same quenching efficiency as the real M molecule, the well depth of the real quenchers $\varepsilon_{PH_2^*-M}/k$ must be equal to the corresponding $\varepsilon_{PH_2^*-Mh}/k$ according to eq 7.

The $\varepsilon_{PH_2^*-M}/k$ values thus obtained are reported in Table 6 where the values for rare gases have however been derived using ε_{M-M}/k literature data of Table 3.

In Figure 6 ln σ has been plotted against these $\varepsilon_{PH_2^*-M}/k$ quantities, the obtained plot reproduces closely the trend of

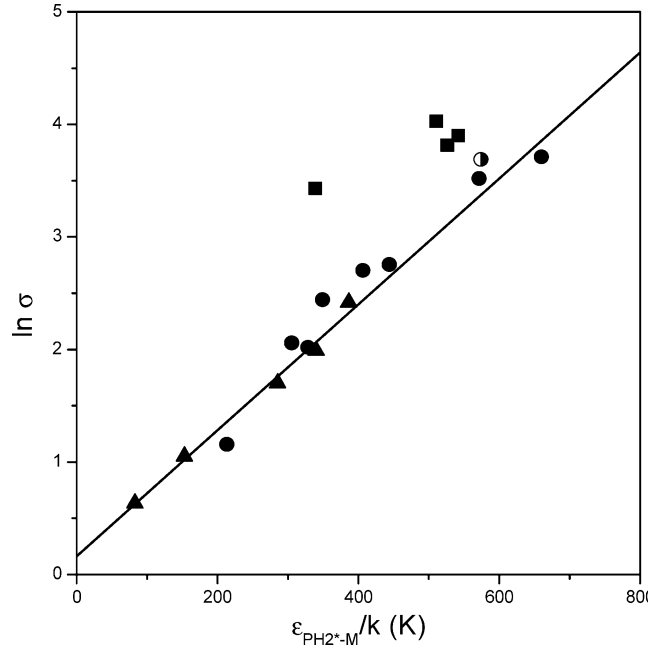

Figure 6. $PH_2(\tilde{A}^2A_1; v_2' = 1)$ quenching: Parmenter et al. plot, ln σ vs $\varepsilon_{PH_2^*-M}/k$; ▲, rare gases; ●, H_2, CH_4, N_2, CO, CO_2, N_2O, COS, and SO_2; ◑, $CHCl_3$; ■, NO, PH_3, NH_3, and H_2S; straight line: linear fitting of rare gas data.

Figure 5 showing definitely that the quenching of $PH_2(\tilde{A}^2A_1)$ due to collisions with the quenchers studied, except NO, PH_3, NH_3, and H_2S, do follow the Parmenter et al. model represented originally by eq 7, prior to the involvement of the combining rule. The slope of the fitting line obtained from only rare gas data is seen to be 0.0063 in agreement with the coefficient 1.67/T, or 0.0056 with $T = 298$ K, of eq 7.

Maximum multipole interactions between $CHCl_3$ and $PH_2(\tilde{A}^2A_1; v_2' = 1)$ give rise to a very high value α_{Mh} for the hypothetical molecule which should simulate $CHCl_3$ in the deactivation of PH_2^*. This value of α_{Mh} should correspond, according to the rare gas line of Figure 5 and through the value of ε_{Mh-Mh}/k of Table 4, to a value of PH_2^* quenching cross section which is not verified by the experimental data. This latter agrees rather well with a polarizability α_{Mh} derived from angle averaged interactions of the collision pair. The size and in particular the mass of $CHCl_3$ might probably hinder the possibility of the two collision partners to settle in the most favorable conditions for interactions during their encounter as in the case of the other quenchers which are mostly much less massive. The fact that $CHCl_3$ interacts with PH_2^* differently from the other quenchers must not be a surprise considering the distinct individuality of each rare gas or molecular species.

IV. Conclusion

The original expression of the Parmenter et al. model is represented by eq 7 which relates the deactivation cross section to the well depth $\varepsilon_{PH_2^*-M}$ of the PH_2^*-M collision complex. $\varepsilon_{PH_2^*-M}$ is notoriously an inaccessible quantity, so it has been replaced, involving the combining rule, by $(\varepsilon_{PH_2^*-PH_2^*})^{1/2}(\varepsilon_{M-M})^{1/2}$ with ε_{M-M} usually found in literature. By this way the process cross section is directly connected to a known molecular property of the quencher.

Figure 1, however, shows that a plot of the experimental values of ln σ against $(\varepsilon_{M-M}/k)^{1/2}$ does not strictly obey the Parmenter et al. correlation eq 9. By simulating the quenching effects of the real quenchers with rare gas-like molecules having

polarizability as sole electric property, we have been through ad hoc built Lennard-Jones type potentials, able to determine the α_{Mh} polarizabilities of these rare gas-like molecules and then the corresponding $(\varepsilon_{Mh-Mh}/k)^{1/2}$. By replotting ln σ vs these $(\varepsilon_{Mh-Mh}/k)^{1/2}$ instead of $(\varepsilon_{M-M}/k)^{1/2}$, eq 9 is seen to be obeyed by all the quenchers except NO, PH_3, NH_3, and H_2S. From the combination of different ε_{Mh-Mh} values with the value of $\varepsilon_{PH_2^*-PH_2^*}$ calculated from rare gas data, we have derived the well depths $\varepsilon_{PH_2^*-M}$ of the collision complexes of $PH_2(\tilde{A}^2A_1)$ with the different real quenchers. A plot of ln σ against $\varepsilon_{PH_2^*-M}/k$ is seen to agree very well with Parmenter et al. eq 7 for all the studied quenchers with the exception of the above-mentioned molecules showing the validity of the Parmenter and co-workers' model in accounting for the process of collisional deactivation of $PH_2(\tilde{A}^2A_1)$.

From what is illustrated above, it is clear that the apparent limited validity of Parmenter and co-workers' theory first observed when ln σ is plotted vs $(\varepsilon_{M-M}/k)^{1/2}$ is due to the fact that the combining rule is not applicable to most quenchers different from rare gases.

We have demonstrated that the molecular quenchers studied, with the exception of NO, PH_3, NH_3, and H_2S, act on the excited $PH_2(\tilde{A}^2A_1)$ species only on a physical basis through their electric properties, dipole and quadrupole moments, and polarizability. Their quenching effects can be assimilated to those of rare gases, then their quenching mechanism should be the same as that of these latter.

In the case of possible dual mechanisms of $PH_2(\tilde{A}^2A_1)$ removal, like probably for NO, PH_3, NH_3, and H_2S, it should be possible to separate the physical mechanism from the chemical one and evaluate their respective contributions to the total quenching cross sections.

The proposed procedure of assimilating the real quenchers with equivalent hypothetical rare-gas-like molecules has also permitted us to have information about the type of multipole interactions, i.e., orientation angle averaged interactions or interactions in most favorable conditions, between the collision partners.

The determination of the collision complex well depths $\varepsilon_{PH_2^*-M}$ is in itself an important result obtained in this work as these quantities can be considered as inaccessible for the fact that PH_2^* is an excited electronic species of a radical.

Preliminary investigations have shown that what we have found with the quenching of $PH_2(\tilde{A}^2A_1)$ seems not specific of this system but also applicable to others.

Acknowledgment. The author wishes to thank Mrs. Fulvia Viri for some technical assistance.

References and Notes

(1) Selwynn, J. E.; Steinfeld, J. I. *Chem. Phys. Lett.* **1969**, *4*, 217.
(2) Thayer, C. A.; Yardley, J. T. *J. Chem. Phys.* **1972**, *57*, 3992.
(3) Holtermann, D. L.; Lee, E. K. C.; Nanes, R. *J. Chem. Phys.* **1982**, *77*, 5327.
(4) Fairchild, P. W.; Smith, G. P.; Crosley, D. R. *J. Chem. Phys.* **1983**, *79*, 1795.
(5) Hofzumahaus, A.; Stuhl, F. *J. Chem. Phys.* **1985**, *82*, 3152.
(6) Lin, H.-M.; Seaver, M.; Tang, K. Y.; Knight, A. E. W.; Parmenter, C. S. *J. Chem. Phys.* **1979**, *70*, 5442.
(7) Parmenter, C. S.; Seaver, M. *J. Chem. Phys.* **1979**, *70*, 5458.
(8) Hirschfelder, J. O.; Curtiss, C. F.; Bird, R. Byron *Molecular Theory of Gases and Liquids*, 4th printing; Wiley: New York, 1967.
(9) Nguyen Xuan, C. *J. Phys. Chem. A* **2007**, *111*, 3216, and references cited therein.
(10) Nguyen Xuan, C.; Margani, A. *Chem. Phys. Lett.* **2000**, *321*, 328.
(11) Smyth, C. P. *Dielectric Behavior and Structure*; McGraw- Hill Book Company, Inc.: New York, 1955.
(12) Herzberg, G. *The Spectra and Structures of Simple Free Radicals*; Cornell University Press: Ithaca, NY, 1971.
(13) Eubank, P. T. *AIChE J.* **1972**, *18*, 454.
(14) Nguyen Xuan, C.; Margani, A.; Mastropietro, M. *J. Chem. Phys.* **1997**, *106*, 8473.

JP903503Z